Quality assurance and quality control of atmospheric organosulfates measured using hydrophilic interaction liquid chromatography (HILIC).

Ping Liu[1,2,4], Xiang Ding[1,3*], Bo-Xuan Li[1], Yu-Qing Zhang[1], Daniel J. Bryant[2*], Xin-Ming Wang[1,3]

[1]State Key Laboratory of Organic Geochemistry and Guangdong Provincial Key Laboratory of Environmental Protection and Resources Utilization, Guangzhou Institute of Geochemistry, Chinese Academy of Sciences, Guangzhou, 510640, China

[2]Wolfson Atmospheric Chemistry Laboratories, Department of Chemistry, University of York, York YO10 5DD, U.K

[3]Guangdong-Hong Kong-Macao Joint Laboratory for Environmental Pollution and Control, Guangzhou Institute of Geochemistry, Chinese Academy of Science, Guangzhou, 510640, China

[4]University of Chinese Academy of Sciences, Beijing, 100049, China

Correspondence to:

Xiang Ding (xiangd@gig.ac.cn)

Daniel J. Bryant (daniel.bryant@york.ac.uk)

Abstract. As a crucial constituent of fine particulate matter ($PM_{2.5}$), secondary organic aerosols (SOA) influence public health, regional air quality, and global climate patterns. This paper highlights the use of Hydrophilic interaction liquid chromatography (HILIC) which effectively retains strongly polar analytes that might exhibit incomplete or no retention in reverse chromatography, resulting in superior separation efficiency.

A HILIC column was used to analyze six standards, environmental standards (1648a and 1649b), and samples collected in urban environments in the Guangzhou of Pearl River Delta region. That serve as valuable reference points for evaluating the organic composition of the atmospheric environment. The results indicate a high degree of accuracy in the analytical method, sodium octyl-d_{17} sulfate serves as the internal standard, with a linear correlation coefficient of the six standards, boasting a linear correlation coefficient r ranging from 0.993-0.9991 and a slope, *k*, of the linear equation from 0.966-1.882. The instrument detection limits (IDLs) are established at 0.03-0.20 $\mu g\ mL^{-1}$, while the method detection limits (MDLs) fall within the range of 0.30-1.75 $ng\ m^{-3}$, demonstrating the method's exceptional sensitivity.

Since isoprene-derived organosulfates (iOSs) are highly polar due to containing a hydrophilic bond to

31   the hydroxyl group and a hydrophobic bond to the sulfate, and as such showed strong retention using this

32   method. This technique employs sodium ethyl sulfate and sodium octyl sulfate standards for semi-

33   quantitative compound analysis iOSs, the error in sample analysis (E_A) ranged from 12.25 %-95.26 %

34   and the two standards maintaining a consistent recovery rate between 116 %-131 % and 86.4 %-127 %.

35   These findings indicate a high level of precision when semi-quantifying compounds with similar

36   structural characteristics, affirming the analysis method's minimal relative error and underscoring its

37   repeatability, process stability, and the reliability of its results for iOSs. To enhance the method's

38   reliability assessment, the study analyzed polar organic components of standard particulate matter

39   samples (1648a and 1649b), providing precise determinations of several iOSs using this method.

40   Methyltetrol sulfate (*m/z* 215, $C_5H_{11}SO_7^-$) is the highest concentration in the ambient samples, up to 67.3

41   ng m^{-3} at daytime. These results serve as valuable reference points for assessing the organic composition

42   of the atmospheric environment.

43   **1. Introduction**

44   Organosulfates (OSs) represent a category of organic compounds featuring the sulfate functional group

45   (R-OSO₃H), found ubiquitously in atmospheric aerosols, OSs contribute to 5-30 % of the organic mass

46   fraction within particulate matter (Shakya and Peltier, 2013; Shakya and Peltier, 2015; Tolocka and

47   Turpin, 2012; Surratt et al., 2008; Lukacs et al., 2009). Their unique hydrophilic and hydrophobic

48   characteristics influence the hygroscopicity and cloud condensation nuclei (CCN) formation potential of

49   aerosol particles (Hansen et al., 2015), underscoring the need for a comprehensive investigation into their

50   chemical compositions and formation mechanisms in the atmosphere. OSs are formed from the oxidation

51   of anthropogenic precursors, such as benzene and toluene and biogenic volatile organic compounds

52   (VOCs) such as isoprene, monoterpenes (primarily α-pinene, β-pinene, and limonene), sesquiterpenes,

53   aromatics, aldehydes, and others, under a variety of oxidation and sulfuric acid conditions (Surratt et al.,

54   2008; Surratt et al., 2010). Isoprene is the most abundant precursor of global secondary organic aerosol

55   (SOA) (Bates and Jacob, 2019; Hodzic et al., 2016). The epoxide pathway plays a critical role in isoprene

56   SOA (iSOA) formation, in which isoprene epoxydiols (IEPOX) and/or hydroxymethyl-methyl-α-lactone

57   (HMML) can react with nucleophilic sulfate producing isoprene-derived organosulfates (iOSs) (Surratt

58   et al., 2010; Lin et al., 2013; He et al., 2018).

Previous research has employed reversed-phase liquid chromatography (RPLC) for the analysis of aqueous atmospheric samples encompassing water-soluble and methanol-extractable aerosol constituents, as well as fog water (Bryant et al., 2020; Bryant et al., 2021). This reversed-phase approach, utilizing a non-polar stationary phase and a polar mobile phase, effectively retains higher-molecular weight OSs derived from monoterpenes (e.g., $C_{10}H_{16}NSO_7^-$) (Gao et al., 2006; Surratt et al., 2007b) and aromatic OSs (e.g., $C_7H_7NSO_4^-$) (Kundu et al., 2010; Staudt et al., 2014). However, it is less efficient for the separation of lower-molecular weight and highly polar OSs, which elute in less than 2.5 min and co-elute with various other OSs, small organic acids, polyols, and inorganic sulfates (Stone et al., 2012). The co-elution of so many analytes leads to matrix effects, reducing the analyte's signal (Bryant et al., 2020; Bryant et al., 2021; Bryant et al., 2023b; Bryant et al., 2023a). The iOSs are hydrophilic compounds owing to their hydroxyl functional groups, and the iOSs are ionic polar compounds. Hence, an alternative approach for the iOSs characterization that could accomplish simultaneous analysis of polar and water-soluble components while avoiding the drawbacks associated with current analytical methods would be highly desirable.

To address this challenge, a Hydrophilic interaction liquid chromatography (HILIC) featuring an amide stationary phase has been utilized (Hettiyadura et al., 2015; Hettiyadura et al., 2017; Cui et al., 2018). HILIC is purposefully designed to retain molecules with ionic and polar functional groups and has demonstrated effectiveness in retaining carboxylic acid-containing OSs like glycolic acid sulfate and lactic acid sulfate, which are among the most prevalent atmospheric OSs quantified to date (Olson et al., 2011; Hettiyadura et al., 2015; Hettiyadura et al., 2017; Cui et al., 2018). Since these OSs compounds are easily ionized in negative mode, they can be efficiently detected in negative electrospray ionization ((−) ESI) mode (Romero and Oehme, 2005; Surratt et al., 2007a). In this experiment, a combination of HILIC chromatographic separation and tandem mass spectrometry (MS/MS) was employed to separate and detect highly polar OSs relevant to the atmosphere. A mixed standard of OSs facilitated the separation, identification, and quantification of polar, ionic, and non-volatile OSs present in the atmosphere. The HILIC separation was accomplished using an ethylene bridged hybrid (BEH) amide column, and OSs were semi-quantified based on the calibration curve derived from alternative standards through triple quadrupole mass spectrometry detection (TQD). This approach enabled the detection and quantification of OSs originating from isoprene within the atmosphere of the Pearl River Delta.

88   Recent studies have identified hundreds of OSs in the ambient environment (Iinuma et al., 2007;

89   Surratt et al., 2008; Riva et al., 2016; Brueggemann et al., 2017; Le Breton et al., 2018; Hettiyadura et

90   al., 2019; Bruggemann et al., 2019). Yet, authentic standards for OSs remain scarce, with only a few

91   commercially available or synthesized in laboratories (Staudt et al., 2014; Hettiyadura et al., 2015; Huang

92   et al., 2018). The utilization of different surrogate standards results in considerable discrepancies in

93   quantifying OS concentrations (Zhang et al., 2022; He et al., 2018; Surratt et al., 2008), signifying the

94   persisting challenge of accurate quantification in OS studies. HILIC chromatography is a promising

95   analytical technique for the separation of OSs from one another and the complex aerosol matrix. When

96   coupled with authentic standard development and highly sensitive MS/MS detection, it offers an

97   improved method for quantifying and speciating atmospheric OSs. Enhanced measurements of this

98   compound class will contribute to a better understanding of SOA precursors and their formation

99   mechanisms.

100   **2 Experimental sections**

101   **2.1 Field Sampling**

102   Sampling was undertaken during October 2018 in Guangzhou, Guangzhou is situated in the Pearl River

103   Delta region of southern China which has large-scale land coverage of broadleaf evergreen trees as well

104   as high-temperature and strong solar radiation all year round.

105   Field sampling was conducted using a $PM_{2.5}$ sampler (Tisch Environmental Inc., Ohio, USA) equipped

106   with quartz filters (Whatman, 17.6 cm. $\times$ 23.4 cm.) at a flow rate of $1.13 m^3 min^{-1}$. Additionally, field

107   blanks were collected at a monthly interval. Blank filters were covered with aluminum foil, and baked at

108   500°C for 24 h to remove organic material, pre- and post- sampling flow rates were measured with a

109   calibrated rotameter. All filters were handled using clean techniques, which included storage of filters in

110   plastic petri dishes lined with pre-cleaned aluminum foil and manipulation with pre-cleaned stainless

111   steel forceps. Post-sampling, filters were stored frozen in the dark. One field blank was collected for

112   every five samples, and stored in a container with silica gel. After sampling, the filter samples were stored

113   at −20°C.

2.2 PM sample extraction and preparation

Following the procedure outlined by Hettiyadura et al. (Hettiyadura et al., 2015), an 82 mm diameter circular section was excised from the quartz membrane using a cutter. This section was subsequently cut into small pieces with forceps that had been cleaned with acetonitrile (ACN). The samples were then carefully placed into a 100 mL clean beaker. To this, 300 μL of a solution with ACN and ultra-pure water (95:5, by volume) containing sodium octyl-d_{17} sulfate at a concentration of 5.3 μg mL^{-1} was introduced as an internal standard. Subsequently, 15 mL of ACN of chromatographic purity and ultrapure water (95:5, by volume) were added in three separate increments, with the beaker was covered with aluminum foil to prevent the organic solvent from evaporating, and extracted by ultra-sonication extraction in an ice water bath for 20 min. The resulting solution was then filtered through a polypropylene membrane syringe filter (0.45 μm; 25 pp, Sigma-Aldrich) and the process was repeated three times to consolidate the solution. The solution was then concentrated to an approximate volume of 5 mL using a rotary evaporator, these were transferred to 1.5 mL vials and the solvent was blown to dryness using a micro-scale nitrogen evaporation system at 35°C under a high-purity nitrogen stream, extracts were then re-constituted with ACN and ultra-pure water (95:5, by volume) to a final volume of 300 μL. The solution was thoroughly mixed and then stored in a freezer at −20°C for subsequent analysis.

2.3 Instrumentation and Reagents

OS sample analysis was performed using ultra-performance liquid chromatography electrospray triple quadrupole tandem mass spectrometry (UPLC/ESI-TQD-MS/MS, Agilent 6400, USA) with a BEH amide column (2.1 mm×100 mm, 1.7 μm; ACQUITYUPLC, Waters) in full-scan mode. The column temperature was held at 35°C and the mobile phase flow rate was 0.5 mL min^{-1}. The injection volume of samples and standards is 5 μL. Mobile phase A (organic phase) with ACN and water (95:5, by volume) buffered with ammonium acetate buffer (10 mm, pH 9) and mobile phase B (aqueous phase) is 100 % water, ammonium acetate buffer (10 mm, pH 9). Use the MassHunter software (version B.02) to acquire and process all data.

Purchased standards: Sodium methyl sulfate (98 %, Sigma-Aldrich), sodium ethyl sulfate (>98 %, Sigma-Aldrich), sodium octyl sulfate (99 %, Alfa Aesar), sodium dodecyl sulfate (99.0 %, Sigma-Aldrich), sodium hexadecyl sulfate (99 %, Alfa Aesar), sodium octadecyl sulfate (99 %, Alfa Aesar), sodium octyl-d_{17} sulfate (99.1 %, CDN), chromatographic pure acetonitrile, (ACN, 99.9 %, CNW),

143 ammonium acetate (99.0 %, CNW), ammonia (20 %-22 %, CNW).

2.4 Separation and detection of OSs

2.4.1 Separation

The separation was optimized using a gradient elution method. Mobile phase A remained at 100 % from 0 to 2 min, after which it decreased to 85 % from 2 to 4 min and remained constant at 85 % until 11 min. To re-equilibrate the column before the next injection, mobile phase A was reinstated to 100 % between 11 and 11.5 min, and this composition was maintained until 20 min. The cleaning needle solvent employed a mixture of acetonitrile and ultrapure water (in a volume ratio of 80:20).

2.4.2 Detection

In the negative ion mode, the identification of OSs was achieved via TQD-MS, specifically utilizing an ACQUITY system as the mass spectrometer (Waters, USA). The detector operated in Full Scan mode, with the first quadrupole selecting deprotonated molecules, the second quadrupole identifying fragments, and the third quadrupole analyzing product ions.

2.4.3 Optimization of experimental conditions

The choice of the fragmentation voltage directly impacts the instrument's ability to target specific compounds, while the collision energy plays a crucial role in determining the extent of fragmentation and the response of secondary fragment ions. To illustrate, when analyzing the most common compounds in the sample, and without connecting the chromatographic separation column, a 5 μL aliquot of the environmental sample was injected every 0.7 min. In this production scanning mode, the target ions generated after ionization in the ion source were detected. The first fragmentation voltage was set at 80 V, and with each subsequent scan, the voltage was incrementally increased by 5 V until it reached 180 V. The analysis revealed that the optimal response was achieved at 135 V. Consequently, 135 V was selected as the optimal fragmentation voltage for quantitative analysis of the actual samples.

For compounds with intricate chemical structures, further analysis was carried out using MS/MS. Similarly, an energy level of 8 eV was employed in the collision cell during the OS daughter ion scanning. Table 1 displays the optimal fragmentation voltage and collision energy for different standards.

The determination of other optimal conditions for the ESI source followed a similar methodology, as

170 presented in Table 2. Include a capillary voltage of 2700 V, source temperature of 150℃, sheath gas

171 temperature of 400℃, source gas (N$_2$) flow rate at 1.7 L min^{-1} and sheath gas (N$_2$) flow rate at 12 L

172 min^{-1}.

173 **Table 1. Optimal fragmentation voltage and collision energy of different standards.**

Compounds	Molecular Weight (MW)	Fragmentation voltage(V)	Collision energy (eV)
Sodium methyl sulfate	134.08	130-150	8-10
Sodium ethyl sulfate	148.11	130-150	8-10
Sodium octyl sulfate	232.27	120	8
Sodium dodecyl sulfate	288.38	130-150	8-10
Sodium hexadecyl sulfate	344.49	130-150	8-10
Sodium octadecyl sulfate	372.54	140	8-10
Sodium octyl-d$_{17}$ sulfate	232.27	120-140	8

174 **Table 2. Other ESI conditions of MS.**

Other ESI sources	Conditions
Source Gas Temp	150℃
Source Gas Flow	1.7 L min^{-1}
Nebulizer	45 psi
Sheath Gas Temp	400℃
Sheath Gas Flow	12 L min^{-1}
Capillary Voltage	2700 V
Nozzle Voltage	500 V
Chamber Current	0.18 μA

175 **3 Results and discussion**

176 **3.1 Comparison of this method and reversed-phase.**

177 **3.1.1 Comparison of OS standards**

178 In this experiment, six OS standards were analyzed. Table 3 compares the retention times and peak areas

179 of pure and mixing standards. The results indicate that the retention times for all standards remained

180 unchanged. Furthermore, there was no co-elution observed between the pure and mixing standards of

7

small molecular weight iOSs, such as $CH_3SO_4^-$ & $C_2H_5SO_4^-$. The peak area ratios of pure to mixing standards were 1.00 and 0.96, respectively. However, co-elution exists for the long-chain alkane OSs ($C_{12}H_{25}SO_4^-$, $C_{16}H_{33}SO_4^-$, $C_{18}H_{37}SO_4^-$), with peak area ratios of 0.57, 0.60, and 0.67, respectively. The mixing standards reduced the signal by almost half, possibly due to a retention time of approximately 0.5 min, falling within the column deadtime.

The ratio of the standards with retention time were 0.8-1 min are close to 1, showing that even though some of the standards closely elute this doesn't effect the instrument response, suggesting no matrix effect. But the long chain OSs, which elute in the dead volume have a large matrix effect. Meaning that the small amount of retention in this method is much better than the no retention in the reverse phase method. This observation suggests that the analytical effectiveness of this method on iOSs with high polarity surpasses that of long-chain alkane OSs.

Table 3. Comparison of retention time and peak aera in MS between pure standards and mixing standards.

Compounds	[M-H]⁻ m/z	[M-H]⁻ Formula	Standards	tR (min)	Peak area	Peak area ratio (Pure/mixing)
Sodium methyl sulfate	111	$CH_3SO_4^-$	pure	0.92	19059629	1.00
			mixing	0.92	19009710	
Sodium ethyl sulfate	125	$C_2H_5SO_4^-$	pure	0.81	15696871	0.96
			mixing	0.81	16315513	
Sodium octyl sulfate	209	$C_8H_{17}SO_4^-$	pure	0.56	44588250	0.86
			mixing	0.56	51744174	
Sodium dodecyl sulfate	265	$C_{12}H_{25}SO_4^-$	pure	0.52	34579898	0.57
			mixing	0.52	60595452	
Sodium hexadecyl sulfate	321	$C_{16}H_{33}SO_4^-$	pure	0.51	31064839	0.60
			mixing	0.51	51815669	
Sodium octadecyl sulfate	349	$C_{18}H_{37}SO_4^-$	pure	0.50	36757474	0.67
			mixing	0.50	55209165	

3.1.2 Comparison of iOSs in ambient sample.

The separation of typical OSs such as $C_5H_{11}SO_7^-$ (m/z 215) and $C_4H_7SO_7^-$ (m/z 199) was notably enhanced using this method, as illustrated in Fig. 1, which compares the separation with the previous

8

196 reversed-phase column. Specifically, for $C_5H_{11}SO_7^-$ (*m/z* 215), the separation of six peaks by this

197 method is superior to reversed-phase chromatography, in which these IEPOX-derived OSs isomers co-

198 elute in two peaks (Stone et al., 2012). The resolution of isomers is significant, because methyltetrol

199 sulfates have generated the greatest OSs signal in prior field studies (Froyd et al., 2010; Lin et al., 2013)

200 and may prove useful in elucidating different OSs formation pathways.
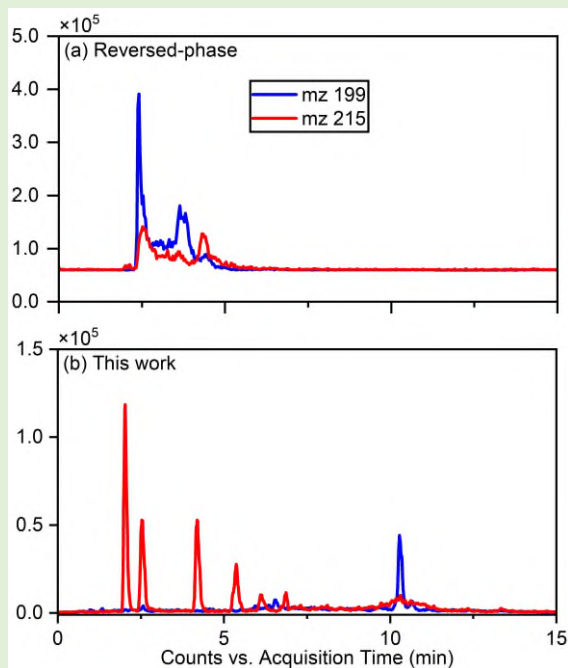
201
202 **Figure 1. Comparison of the effects of separation of *m/z* 199 ($C_4H_7SO_7^-$) and *m/z* 215 ($C_5H_{11}SO_7^-$) using the**
203 **previous method and this work.**

204 Due to co-eluting effects, the retention time for *m/z* 139, 153, 155, 167 and 169 under the traditional

205 method was 1.30 min (Stone et al., 2012). However, employing the HILIC method, significant shifts in

206 retention times were observed. Specifically, retention times for *m/z* 139 were 0.83 & 1.58 min, *m/z* 153

207 were 0.79 & 0.82 min, for *m/z* 155, 167, and 169 were 10.48, 0.69 & 1.00 and 1.46 min respectively.

208 Additionally, Fig. 2 displays chromatograms of iOSs with retention times of less than 1 min, while some

209 co-elution persists, their retention times do not precisely overlap. This observation underscores the

210 method's potential for effectively separating lower molecular weight and highly polar OSs.
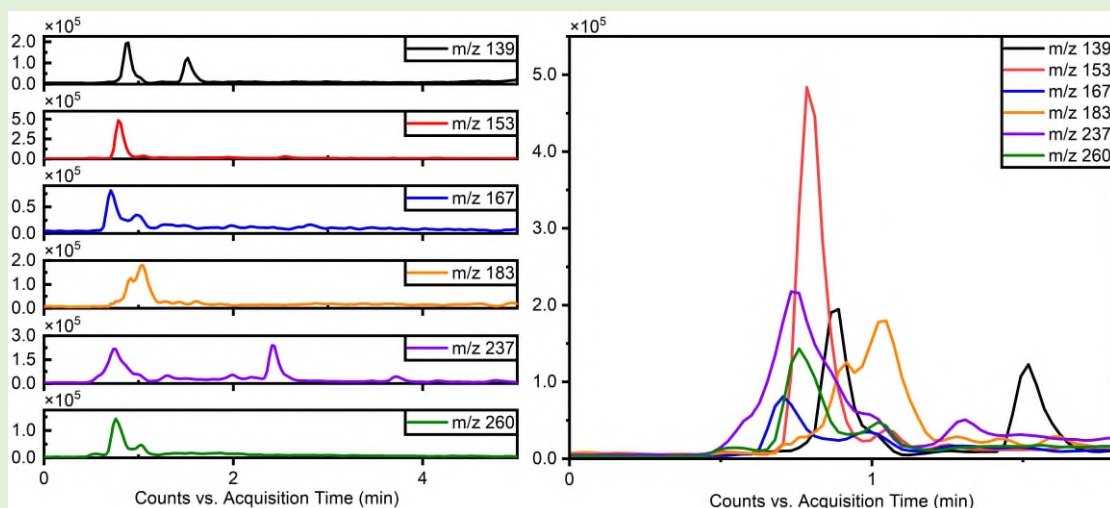
Figure 2. Chromatograms of iOSs with retention times less than 1 min.

3.2 Linearity of the standard

In this experiment, the sodium octyl-d$_{17}$ sulfate standard solution (300 µL; 5.3 µg mL^{-1}) as an internal standard, six commercially available OS standards were employed. Table 4 and Fig. 3 present the linearity for different standards. The standard curves of various compounds were evaluated for their correlation coefficients (r), resulting in values ranging from 0.993 to 0.9991, the resulting slope (k) ranging from 0.966-1.882, and the Pearson significance test (p) indicating values ≤ 0.002. Notably, the standard curve for sodium octyl sulfate (m/z 209, $C_8H_{17}SO_4^-$) exhibited a r of 0.9991, with a k of 0.966, indicating that the semi-quantification of structurally similar compounds using sodium octyl sulfate as the standard was more precise when sodium octyl-d$_{17}$ sulfate was used as the internal standard.

Table 4. The Linear of standards. k is the slope of correlation, r is the correlation coefficient, p is the Pearson significance test.

Compounds	[M-H]$^-$		tR（min）	k	r	p
	m/z	Formula				
Sodium methyl sulfate	111	$CH_3SO_4^-$	1.06	1.499	0.998	<0.001
Sodium ethyl sulfate	125	$C_2H_5SO_4^-$	0.95	1.185	0.993	0.002
Sodium octyl sulfate	209	$C_8H_{17}SO_4^-$	0.63	0.966	0.9991	<0.001
Sodium dodecyl sulfate	265	$C_{12}H_{25}SO_4^-$	0.58	1.484	0.994	<0.001
Sodium hexadecyl sulfate	321	$C_{16}H_{33}SO_4^-$	0.57	1.882	0.996	<0.001
Sodium octadecyl sulfate	349	$C_{18}H_{37}SO_4^-$	0.56	1.336	0.998	<0.001

3.3 UPLC/ESI–MS/MS instrument detection limits and method detection limits

To ensure the effectiveness of this method in monitoring the target compounds in field environmental samples, the standard deviation (SD) was computed by repeatedly injecting the standard sample with the lowest concentration five times in succession, the calculation used the standard curve of Fig. 3.
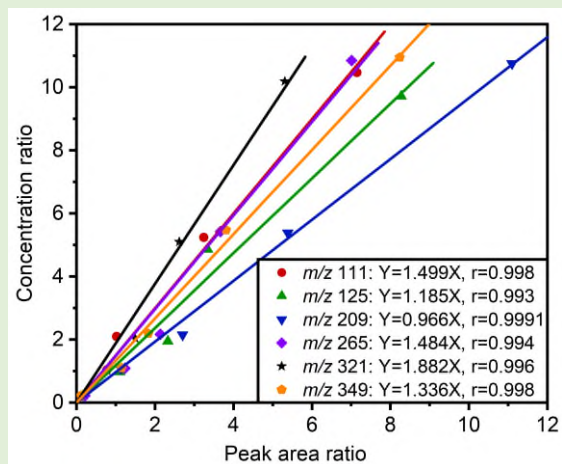
Figure 3. Correlations between concentration ratios and area ratios of standards to the internal standard, r is the correlation coefficient.

The instrumental detection limits (IDLs) were established at the 95 % confidence interval, calculated as 3 times SD divided by 'k'. In this experiment, with a sample sampling volume of 271.2 m^3 and considering the entire laboratory analysis process, the method detection limits (MDLs) for these compounds were determined, calculated following Eq. (1)- Eq. (2):

$$MDLs = IDLs * \frac{V_1}{V_2} \tag{1}$$

$$V_2 = V_0 * \frac{S_1}{S_2} \tag{2}$$

Where the area of a sampling filter (82mm diameter) for OS analysis (S$_1$) was 52.78 cm^2, and the total area of a sampling filter (S$_2$) was 411.84 cm^2. The total air volume of 4 h sampling at a flow rate of 1.13 m^3 min^{-1} (V$_0$) was 271.2 m^3, the solution volume in the vial for LC/MS analysis (V$_1$) was 300 μL, which same as the internal standard added, and the air volume responding to the filter analyzed (V$_2$) was 34.76 m^3.

The MDLs of each as standard depicted in Table 5. Of the various standard samples analyzed, the compound with the highest method detection limit was sodium dodecyl sulfate, which measured at 1.75 ng m^{-3}. This finding underscores the method's remarkable sensitivity in detecting OSs in environmental aerosols, thereby affirming its effective detection capability.

Table 5. The IDLs: Instrumental detection limits (µg mL^{-1}). MDLs: Method detection limits (ng m^{-3}). M:

Sample concentration (µg mL^{-1}), total sampling 5 times. SD: Standard deviation.

Standards	M$_1$	M$_2$	M$_3$	M$_4$	M$_5$	SD	IDLs (µg mL^{-1})	MDLs (ng m^{-3})
Sodium methyl sulfate	0.08	0.08	0.06	0.08	0.11	0.02	0.03	0.30
Sodium ethyl sulfate	0.11	0.14	0.09	0.14	0.17	0.03	0.08	0.67
Sodium octyl sulfate	0.07	0.07	0.05	0.07	0.06	0.01	0.04	0.30
Sodium dodecyl sulfate	0.12	0.25	0.09	0.18	0.34	0.10	0.20	1.75
Sodium hexadecyl sulfate	0.14	0.16	0.06	0.19	0.15	0.05	0.08	0.66
Sodium octadecyl sulfate	0.09	0.14	0.15	0.16	0.26	0.06	0.14	1.23

3.4 Parallelism and recovery

In this experiment, a matrix spike experiment was conducted. Approximately 300 µL of a mixed solution, containing all the standards at a concentration of around 5 µg mL^{-1}, was injected onto a 47 mm blank quartz membrane. This procedure was repeated in parallel five times, and a sample without the mixed solution served as a laboratory blank, adding up to a total of six sample groups for pretreatment analysis. The total quantity of each substance in the treated sample and the content of each substance in the untreated sample were computed, thereby enabling the calculation of the recovery rate for each compound. As demonstrated in Table 6, the recovery rates for various compounds fell within the range of 60.2 % - 145 %. These high recovery rates indicate minimal loss of the target compounds during the analysis, which is favourable for accurate detection.

Moreover, it is noteworthy that the Relative standard deviations (RSDs) for these standards did not surpass 15 %, underscoring the small relative error and highlighting the experiment's reproducibility. The RSDs of the small molecule were all less than 4.4 %, but the RSDs for long-chain alkane OSs are all higher than 10 %, this indicating that this experiment is favourable for the detection of iOSs. The stability of the analysis process ensures that the results obtained are reliable.

Table 6. The recovery and RSD of standards. M: Sample recovery (%).

Compounds	M$_1$(%)	M$_2$(%)	M$_3$(%)	M$_4$(%)	M$_5$(%)	RSD (%)
Sodium methyl sulfate	61.4	64.6	60.3	61.5	60.2	3.0

Sodium ethyl sulfate	128	131	116	123	126	4.4
Sodium octyl sulfate	127	101	106	109	86.4	13
Sodium dodecyl sulfate	145	132	112	113	100	15
Sodium hexadecyl sulfate	121	119	114	115	87.9	12
Sodium octadecyl sulfate	117	95.0	108	86.7	84.4	14

3.5 Empirical approach to estimate error in sample analysis

Stone et al. (Stone et al., 2012) developed an empirical approach to estimate the error resulting from surrogate quantification (E_Q) based on a homologous series of atmospherically relevant compounds. They estimated the relative error introduced by each carbon atom (E_n), oxygenated functional group (E_f), and alkenes (E_d) to be 15 %, 10 %, and 60 %, respectively. The errors introduced by surrogate quantification are considered additive and are calculated as follows. Furthermore, the error in sample analysis (E_A) can be estimated through the error propagation of field blank (E_{FB}), spike recovery (E_R), relative differences (E_D), and the surrogate quantification (E_Q) calculated following Eq. (3). The error in sample analysis (E_A) calculated following Eq. (4):

$$\%E_Q = \%E_n \Delta n + \%E_f \Delta f + \%E_d \Delta d \tag{3}$$

$$\%E_A = \sqrt{(\%E_{FB})^2 + (\%E_R)^2 + (\%E_D)^2 + (\%E_Q)^2} \ldots \tag{4}$$

Where Δn represents the difference in the number of carbon atoms between a surrogate and an analyte, Δf is the difference in oxygen-containing functional groups between a surrogate and an analyte, and Δd is the difference in alkene functionality between a surrogate and an analyte. As shown in Table 7, the E_Q ranged from 10 % to 95 % for the OSs when using sodium ethyl sulfate and sodium octyl sulfate as the surrogates. The E_Q values were compared to the previous surrogate with camphorsulfonic acid, there is 215 % and 230 % reduced to 75 % and 60 % for m/z 215 and m/z 199, respectively (Zhang et al., 2022). And E_A ranged from 12.25 %-95.26 % for these iOS products. For m/z 215 and m/z 199, E_A are 73.33 % and 60.42 %, respectively.

Table 7. Uncertainty associated with sample analysis.

[M-H]$^-$		Surrogate Standards	[M-H]$^-$	E_Q(%)	E_A(%)
m/z	Formula		Standards formula		
139	$C_2H_3SO_5^-$	Sodium ethyl sulfate	$C_2H_5SO_4^-$	10	12.25

153	$C_3H_5SO_5^-$	Sodium ethyl sulfate	$C_2H_5SO_4^-$	25	25.98
155	$C_2H_3SO_6^-$	Sodium ethyl sulfate	$C_2H_5SO_4^-$	20	21.21
167	$C_4H_7SO_5^-$	Sodium ethyl sulfate	$C_2H_5SO_4^-$	40	40.62
169	$C_3H_5SO_6^-$	Sodium ethyl sulfate	$C_2H_5SO_4^-$	35	35.71
183	$C_4H_7SO_6^-$	Sodium ethyl sulfate	$C_2H_5SO_4^-$	50	50.50
199	$C_4H_7SO_7^-$	Sodium octyl sulfate	$C_8H_{17}SO_4^-$	60	60.42
215	$C_5H_{11}SO_7^-$	Sodium octyl sulfate	$C_8H_{17}SO_4^-$	75	75.33
237	$C_7H_9SO_7^-$	Sodium octyl sulfate	$C_8H_{17}SO_4^-$	45	45.55
260	$C_5H_{10}NSO_9^-$	Sodium octyl sulfate	$C_8H_{17}SO_4^-$	95	95.26

284   **3.6 MS^2 of iOSs**

285   In this experiment, the semi-quantitative determination of iOSs was carried out using sodium octyl-d_{17}

286   sulfate as the internal standard, sodium ethyl sulfate and sodium octyl sulfate as the standards. Semi-

287   quantitative analytical methods were employed to monitor the characteristic product ions of OSs (Stone

288   et al., 2009), namely HSO_4^- (*m/z* 97) and $\cdot SO_4^-$ (*m/z* 96). MS^2 was utilized as a means of identifying

289   OSs and performing semi-quantitative analysis when actual standards were not available.

290   Given the wide array of polar compounds present in field samples and the substantial variations

291   between samples, the final qualitative and quantitative analysis was carried out in full-scan mode. This

292   approach ensured the most comprehensive component analysis results. By evaluating the relative signal

293   intensity using HILIC- TQD, it was possible to identify certain OSs. As shown in Fig. 4, we identified a

294   total of 10 OSs, by daughter ion scanning mode. In Fig. 4, only one isomer's MS^2 is listed for reference.
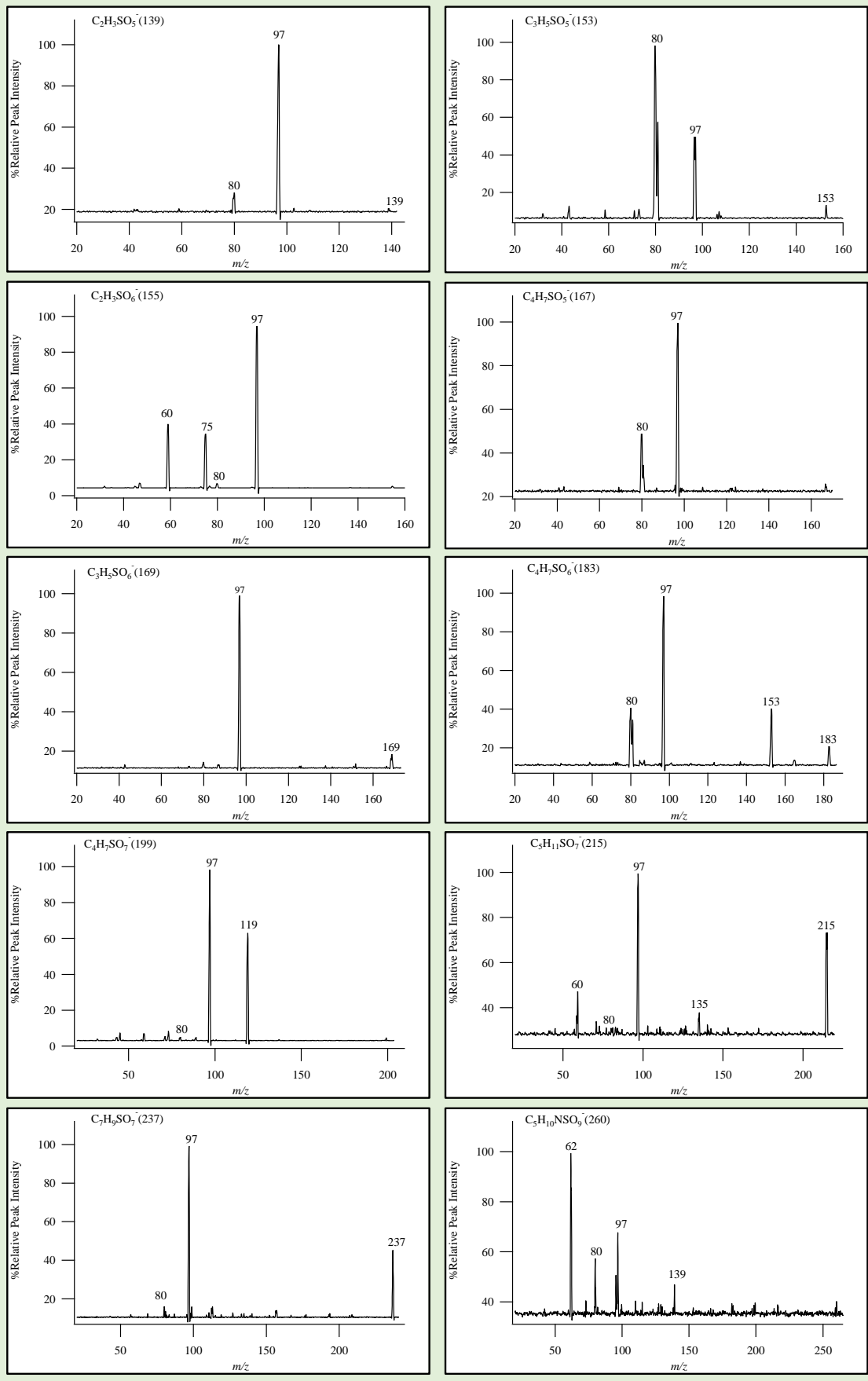
295

296   **Figure 4. MS² TICs of iOSs.**

15

3.7 Measurement of environmental standards

The relatively pristine nature of the standard mixture solution stands in stark contrast to the actual field ambient atmospheric aerosol samples, which are characterized by complex matrices that can significantly influence the analytical results. To comprehensively assess the reliability of this analytical method, we acquired standard particulate matter samples (NIST 1648a and 1649b). We proceeded to analyze the organic components within these samples and determine the content of environmental standard particle samples using the same method. The results, as presented in Tables 8 and 9, among them, the retention time for iOSs is all greater than the deadtime of the column, indicating that the method provides good retention and separation for highly polar iOSs, and reveal that the RSD in the analysis of all compounds does not exceed 27 %. This level of deviation falls within the acceptable range for the analysis of organic compounds, affirming the method's suitability for field sample analysis. These results serve as valuable reference points for assessing the organic composition of the atmospheric environment.

Table 8. The compounds in 1648a. M: Sample concentration (ng m^{-3}).

m/z	$[M-H]^{-1}$ Formula	M_1	M_2	M_3	M_4	M_5	Average	tR（min）	RSD
139	$(C_2H_3SO_5^-)$	15.0	17.8	14.7	13.0	14.0	14.9	0.83, 1.58	12%
153	$(C_3H_5SO_5^-)$	26.6	29.1	24.7	23.7	24.8	25.77	0.79, 0.82	8.3%
155	$(C_2H_3SO_6^-)$	1.83	1.94	1.76	1.78	1.42	1.75	10.48	11%
167	$(C_4H_7SO_5^-)$	17.3	15.8	14.6	14.3	155	15.5	0.69, 1.00	7.6%
169	$(C_3H_5SO_6^-)$	1.58	1.90	1.57	1.27	1.53	1.57	1.46	14%
183	$(C_4H_7SO_6^-)$	9.30	10.1	8.31	7.97	8.69	8.86	0.86, 1.10	9.3%
199	$(C_4H_7SO_7^-)$	5.62	6.71	6.18	5.49	5.77	5.95	10.22	8.3%
215	$(C_5H_{11}SO_7^-)$	70.0	84.5	81.4	68.0	79.9	76.8	1.83, 2.34, 4.25, 5.24, 6.07, 6.54	9.5%
237	$(C_7H_9SO_7^-)$	7.02	8.51	8.20	7.49	7.55	7.55	0.71, 2.54	7.7%
260	$(C_5H_{10}NSO_9^-)$	7.95	11.0	6.06	6.00	7.18	7.63	0.65, 1.02	27%

Table 9. The compounds in 1649b. M: Sample concentration (ng m^{-3}).

m/z	$[M-H]^-$ Formula	M_1	M_2	M_3	M_4	M_5	Average	tR（min）	RSD
139	$(C_2H_3SO_5^-)$	22.5	26.2	24.2	25.0	22.4	24.1	0.83, 1.58	6.8%

16

153	$(C_3H_5SO_5^-)$	37.7	36.6	39.9	39.8	35.1	37.8	0.79, 0.82	5.4%
155	$(C_2H_3SO_6^-)$	2.24	2.08	2.24	2.28	1.88	2.15	10.48	7.8%
167	$(C_4H_7SO_5^-)$	22.2	23.1	23.8	23.5	20.6	22.7	0.69, 1.00	5.7%
169	$(C_3H_5SO_6^-)$	1.99	2.42	2.73	2.42	2.34	2.38	1.46	11%
183	$(C_4H_7SO_6^-)$	7.22	8.78	8.12	8.27	7.79	8.04	0.86, 1.10	7.2%
199	$(C_4H_7SO_7^-)$	8.04	8.11	8.04	7.16	6.67	4.40	10.22	8.6%
215	$(C_5H_{11}SO_7^-)$	98.6	131	114	115	106	113	1.83, 2.34, 4.25, 5.24, 6.07, 6.54	11%
237	$(C_7H_9SO_7^-)$	9.14	11.7	9.23	10.7	9.86	10.1	0.71, 2.54	11%
260	$(C_5H_{10}NSO_9^-)$	3.06	3.36	3.75	3.25	3.13	3.31	0.65, 1.02	8.2%

3.8 iOSs in ambient PM samples

Concentrations of iOSs quantified in ambient PM$_{2.5}$ from Guangzhou in October 2018 daytime and nighttime, are provided in Table 10. Methyltetrol sulfate (m/z 215, $C_5H_{11}SO_7^-$) is the most prevalent OS known to date (Surratt et al., 2008; Hettiyadura et al., 2015). It is formed through a nucleophilic addition reaction involving an IEPOX ring, catalyzed by sulfuric acid (Surratt, Chan et al. 2010). $C_5H_{11}SO_7^-$ (m/z 215) exhibited peak retention times of 1.83, 2.34, 4.25, 5.24, 6.07 and 6.54 min and was the most abundant OS measured. On 7th October during the daytime and 7th-8th October during the nighttime, its concentrations were 67.3 ng m^{-3} and 57.9 ng m^{-3}, respectively.

The OS with formular m/z 260 ($C_5H_{10}NSO_9^-$) is a nitroxic OS resulting from the photooxidation of isoprene under high NOx conditions (Gomez-Gonzalez et al., 2008; Surratt et al., 2008). In the course of this experiment, two isomers with an m/z 260 were discovered, with Hettiyadura and colleagues identifying two such isomers in 2019 (Hettiyadura et al., 2019), and Centreville identifying four isomers with m/z 260 (Surratt et al., 2008). And an m/z 260 exhibits a moderate correlation with methyltetrol sulfate, hinting at isoprene as a likely precursor (Hettiyadura et al., 2019). In this experiment, the concentration of m/z 260 was significantly higher at night than during the day, were 17.5 ng m^{-3} and 10.2 ng m^{-3}, respectively. Further subsequent experiments could explore the reasons for this diurnal difference in terms of the mechanism of formation of m/z 260.

OS with the formulas $C_4H_7SO_7^-$ (m/z 199, calculated mass: 198.9912) is an oxidation product of isoprene under high NOx conditions. In this method, the retention time for the peak is 10.22 min, and the concentration of m/z 199 was significantly higher at night than during the day, were 18.1 ng m^{-3} and 12.5

331   ng m^{-3}, respectively, suggesting that nighttime chemistry is more conducive to the formation of m/z 199.

332   In summary, these findings strongly suggest that isoprene serves as the primary and most abundant

333   precursor to OSs. Hettiyadura et al. (Hettiyadura et al., 2019) demonstrated that during the Atlanta

334   summer, over half of the organic aerosol compounds derived from isoprene are composed of OSs, with

335   methyltetrol sulfate being the predominant constituent. Subsequent experiments can further explore the

336   different formation mechanisms of these iOSs and the reasons for the variations in different isomers.

337 **Table 10. Ambient concentrations of iOSs measured in PM$_{2.5}$ at Guangzhou, from 06:00-18:00 on 7/10/2018**

338 **(daytime) and 18:00-06:00 on 7/10/2018-8/10/2018 (nighttime).**

[M-H]$^-$			tR (min)	Time	Concentration(ng m^{-3})
m/z	Formula	Monoisotopic Mass			
139	$C_2H_3SO_5^-$	138.9701	0.83, 1.58	Daytime	7.70
				Nighttime	9.16
153	$C_3H_5SO_5^-$	152.9858	0.79, 0.82	Daytime	20.9
				Nighttime	34.9
155	$C_2H_3SO_6^-$	154.9650	10.48	Daytime	13.8
				Nighttime	18.7
167	$C_4H_7SO_5^-$	167.0014	0.69, 1.00	Daytime	4.82
				Nighttime	7.66
169	$C_3H_5SO_6^-$	168.9807	1.46	Daytime	11.0
				Nighttime	11.7
183	$C_4H_7SO_6^-$	182.9963	0.86, 1.10	Daytime	8.80
				Nighttime	8.69
199	$C_4H_7SO_7^-$	198.9912	10.22	Daytime	12.5
				Nighttime	18.1
215	$C_5H_{11}SO_7^-$	215.0225	1.83, 2.34, 4.25, 5.24, 6.07, 6.54	Daytime	67.3
				Nighttime	57.9
237	$C_7H_9SO_7^-$	237.0069	0.71, 2.54	Daytime	11.0
				Nighttime	15.4
260	$C_5H_{10}NSO_9^-$	260.0076	0.65, 1.02	Daytime	10.2

		Nighttime	17.5

4 Conclusion

OSs are a vital component of SOA. Previously, their measurement using reversed-phase liquid chromatography presented challenges due to a lack of retention and subsequent co-elution with other organic sulfates, small organic acids, polyols, and inorganic ions, resulting in poor separation and matrix effects. In this experiment, we employed HILIC to analyze OSs in the atmospheric environment. HILIC effectively resolved this issue by delaying the elution time of molecules with ionic and polar functional groups, particularly OSs containing carboxyl groups. HILIC retained strongly polar samples that had incomplete or no retention in C18 reverse chromatography, offering a solution to the co-elution problem of OSs with other small compounds in C18 reverse columns, resulting in a robust separation. Specifically, for $C_5H_{11}SO_7^-$ (m/z 215), the separation of six peaks by this method is superior to reversed-phase chromatography, in which these IEPOX-derived OSs isomers co-elute in two peaks.

During this experiment, we conducted iOSs in the atmospheric environment of the Pearl River Delta using HILIC. And our analytical method possessed high sensitivity, enabling effective detection of OSs in environmental aerosols. Each standard exhibited RSD controlled within 15 %, indicating minimal relative errors, high experimental reproducibility, stable analysis procedures, and reliable results. We also simultaneously analyzed two environmental reference standards (NIST 1648a and 1649b), providing some reference for the quantification of atmospheric OSs.

Nonetheless, research on OSs commenced relatively late, and due to their wide diversity and demanding laboratory synthesis conditions, only a limited number of commercial reference materials are available for quantitative OSs analysis. Consequently, the lack of actual standards led us to employ semi-quantitative analysis methods in this experiment, introducing some uncertainty in quantification. Future work should focus on enhancing the quantitative methods for OSs, utilizing actual standards for one-to-one compound quantification, and refining the measurement techniques for OSs. These efforts will contribute to a deeper understanding of SOA precursors, formation mechanisms, and the contribution of OSs to atmospheric aerosols, ultimately guiding research in the field of air pollution prevention and control.

References

Bates, K. H. and Jacob, D. J.: A new model mechanism for atmospheric oxidation of isoprene: global effects on oxidants, nitrogen oxides, organic products, and secondary organic aerosol, Atmos. Chem. Phys., 19, 9613-9640, http://doi.org/10.5194/acp-19-9613-2019, 2019.

Brueggemann, M., Poulain, L., Held, A., Stelzer, T., Zuth, C., Richters, S., Mutzel, A., van Pinxteren, D., Iinuma, Y., Katkevica, S., Rabe, R., Herrmann, H., and Hoffmann, T.: Real-time detection of highly oxidized organosulfates and BSOA marker compounds during the F-BEACh 2014 field study, Atmospheric Chemistry and Physics, 17, 1453-1469, http://doi.org/10.5194/acp-17-1453-2017, 2017.

Bruggemann, M., van Pinxteren, D., Wang, Y. C., Yu, J. Z., and Herrmann, H.: Quantification of known and unknown terpenoid organosulfates in PM10 using untargeted LC-HRMS/MS: contrasting summertime rural Germany and the North China Plain, Environ. Chem., 16, 333-346, http://doi.org/10.1071/en19089, 2019.

Bryant, D. J., Mayhew, A. W., Pereira, K. L., Budisulistiorini, S. H., Prior, C., Unsworth, W., Topping, D. O., Rickard, A. R., and Hamilton, J. F.: Overcoming the lack of authentic standards for the quantification of biogenic secondary organic aerosol markers, Environmental Science: Atmospheres, 3, 221-229, http://doi.org/10.1039/D2EA00074A, 2023a.

Bryant, D. J., Elzein, A., Newland, M., White, E., Swift, S., Watkins, A., Deng, W., Song, W., Wang, S., Zhang, Y., Wang, X., Rickard, A. R., and Hamilton, J. F.: Importance of Oxidants and Temperature in the Formation of Biogenic Organosulfates and Nitrooxy Organosulfates, ACS Earth and Space Chemistry, 5, 2291-2306, http://doi.org/10.1021/acsearthspacechem.1c00204, 2021.

Bryant, D. J., Nelson, B. S., Swift, S. J., Budisulistiorini, S. H., Drysdale, W. S., Vaughan, A. R., Newland, M. J., Hopkins, J. R., Cash, J. M., Langford, B., Nemitz, E., Acton, W. J. F., Hewitt, C. N., Mandal, T., Gurjar, B. R., Shivani, Gadi, R., Lee, J. D., Rickard, A. R., and Hamilton, J. F.: Biogenic and

394   anthropogenic sources of isoprene and monoterpenes and their secondary organic aerosol in Delhi, India,

395   Atmos. Chem. Phys., 23, 61-83, http://doi.org/10.5194/acp-23-61-2023, 2023b.

396   Bryant, D. J., Dixon, W. J., Hopkins, J. R., Dunmore, R. E., Pereira, K., Shaw, M., Squires, F. A., Bannan,

397   T. J., Mehra, A., Worrall, S. D., Bacak, A., Coe, H., Percival, C. J., Whalley, L. K., Heard, D. E., Slater,

398   E. J., Ouyang, B., Cui, T. Q., Surratt, J. D., Liu, D., Shi, Z. B., Harrison, R., Sun, Y. L., Xu, W. Q., Lewis,

399   A. C., Lee, J. D., Rickard, A. R., and Hamilton, J. F.: Strong anthropogenic control of secondary organic

400   aerosol formation from isoprene in Beijing, Atmospheric Chemistry and Physics, 20, 7531-7552,

401   http://doi.org/10.5194/acp-20-7531-2020, 2020.

402   Cui, T. Q., Zeng, Z. X., dos Santos, E. O., Zhang, Z. F., Chen, Y. Z., Zhang, Y., Rose, C. A.,

403   Budisulistiorini, S. H., Collins, L. B., Bodnar, W. M., de Souza, R. A. F., Martin, S. T., Machado, C. M.

404   D., Turpin, B. J., Gold, A., Ault, A. P., and Surratt, J. D.: Development of a hydrophilic interaction liquid

405   chromatography (HILIC) method for the chemical characterization of water-soluble isoprene epoxydiol

406   (IEPOX)-derived secondary organic aerosol, Environ. Sci.-Process Impacts, 20, 1524-1536,

407   http://doi.org/10.1039/c8em00308d, 2018.

408   Froyd, K. D., Murphy, S. M., Murphy, D. M., de Gouw, J. A., Eddingsaas, N. C., and Wennberg, P. O.:

409   Contribution of isoprene-derived organosulfates to free tropospheric aerosol mass, Proceedings of the

410   National Academy of Sciences of the United States of America, 107, 21360-21365,

411   http://doi.org/10.1073/pnas.1012561107, 2010.

412   Gao, S., Surratt, J. D., Knipping, E. M., Edgerton, E. S., Shahgholi, M., and Seinfeld, J. H.:

413   Characterization of polar organic components in fine aerosols in the southeastern United States: Identity,

414   origin, and evolution, Journal of Geophysical Research-Atmospheres, 111,

415   http://doi.org/10.1029/2005jd006601, 2006.

416   Gomez-Gonzalez, Y., Surratt, J. D., Cuyckens, F., Szmigielski, R., Vermeylen, R., Jaoui, M.,

417   Lewandowski, M., Offenberg, J. H., Kleindienst, T. E., Edney, E. O., Blockhuys, F., Van Alsenoy, C.,

418   Maenhaut, W., and Claeys, M.: Characterization of organosulfates from the photooxidation of isoprene

419   and unsaturated fatty acids in ambient aerosol using liquid chromatography/(-) electrospray ionization

420   mass spectrometry, Journal of Mass Spectrometry, 43, 371-382, http://doi.org/10.1002/jms.1329, 2008.

421   Hansen, A. M. K., Hong, J., Raatikainen, T., Kristensen, K., Ylisirnio, A., Virtanen, A., Petaja, T., Glasius,

422   M., and Prisle, N. L.: Hygroscopic properties and cloud condensation nuclei activation of limonene-

derived organosulfates and their mixtures with ammonium sulfate, Atmospheric Chemistry and Physics, 15, 14071-14089, http://doi.org/10.5194/acp-15-14071-2015, 2015.

He, Q. F., Ding, X., Fu, X. X., Zhang, Y. Q., Wang, J. Q., Liu, Y. X., Tang, M. J., Wang, X. M., and Rudich, Y.: Secondary Organic Aerosol Formation From Isoprene Epoxides in the Pearl River Delta, South China: IEPOX- and HMML-Derived Tracers, Journal of Geophysical Research: Atmospheres, 123, 6999-7012, http://doi.org/10.1029/2017jd028242, 2018.

Hettiyadura, A. P. S., Al-Naiema, I. M., Hughes, D. D., Fang, T., and Stone, E. A.: Organosulfates in Atlanta, Georgia: anthropogenic influences on biogenic secondary organic aerosol formation, Atmospheric Chemistry and Physics, 19, 3191-3206, http://doi.org/10.5194/acp-19-3191-2019, 2019.

Hettiyadura, A. P. S., Stone, E. A., Kundu, S., Baker, Z., Geddes, E., Richards, K., and Humphry, T.: Determination of atmospheric organosulfates using HILIC chromatography with MS detection, Atmospheric Measurement Techniques, 8, 2347-2358, http://doi.org/10.5194/amt-8-2347-2015, 2015.

Hettiyadura, A. P. S., Jayarathne, T., Baumann, K., Goldstein, A. H., de Gouw, J. A., Koss, A., Keutsch, F. N., Skog, K., and Stone, E. A.: Qualitative and quantitative analysis of atmospheric organosulfates in Centreville, Alabama, Atmospheric Chemistry and Physics, 17, 1343-1359, http://doi.org/10.5194/acp-17-1343-2017, 2017.

Hodzic, A., Kasibhatla, P. S., Jo, D. S., Cappa, C. D., Jimenez, J. L., Madronich, S., and Park, R. J.: Rethinking the global secondary organic aerosol (SOA) budget: stronger production, faster removal, shorter lifetime, Atmos. Chem. Phys., 16, 7917-7941, http://doi.org/10.5194/acp-16-7917-2016, 2016.

Huang, R.-J., Cao, J., Chen, Y., Yang, L., Shen, J., You, Q., Wang, K., Lin, C., Xu, W., Gao, B., Li, Y., Chen, Q., Hoffmann, T., amp, apos, Dowd, C. D., Bilde, M., and Glasius, M.: Organosulfates in atmospheric aerosol: synthesis and quantitative analysis of PM2.5 from Xi'an, northwestern China, Atmospheric Measurement Techniques, 11, 3447-3456, http://doi.org/10.5194/amt-11-3447-2018, 2018.

Iinuma, Y., Mueller, C., Boege, O., Gnauk, T., and Herrmann, H.: The formation of organic sulfate esters in the limonene ozonolysis secondary organic aerosol (SOA) under acidic conditions, Atmospheric Environment, 41, 5571-5583, http://doi.org/10.1016/j.atmosenv.2007.03.007, 2007.

Kundu, S., Kawamura, K., Andreae, T. W., Hoffer, A., and Andreae, M. O.: Diurnal variation in the water-soluble inorganic ions, organic carbon and isotopic compositions of total carbon and nitrogen in biomass burning aerosols from the LBA-SMOCC campaign in Rondonia, Brazil, Journal of Aerosol Science, 41,

118-133, http://doi.org/10.1016/j.jaerosci.2009.08.006, 2010.

Le Breton, M., Wang, Y. J., Hallquist, A. M., Pathak, R. K., Zheng, J., Yang, Y. D., Shang, D. J., Glasius, M., Bannan, T. J., Liu, Q. Y., Chan, C. K., Percival, C. J., Zhu, W. F., Lou, S. R., Topping, D., Wang, Y. C., Yu, J. Z., Lu, K. D., Guo, S., Hu, M., and Hallquist, M.: Online gas- and particle-phase measurements of organosulfates, organosulfonates and nitrooxy organosulfates in Beijing utilizing a FIGAERO ToF-CIMS, Atmospheric Chemistry and Physics, 18, 10355-10371, http://doi.org/10.5194/acp-18-10355-2018, 2018.

Lin, Y. H., Knipping, E. M., Edgerton, E. S., Shaw, S. L., and Surratt, J. D.: Investigating the influences of SO2 and NH3 levels on isoprene-derived secondary organic aerosol formation using conditional sampling approaches, Atmospheric Chemistry and Physics, 13, 8457-8470, http://doi.org/10.5194/acp-13-8457-2013, 2013.

Lukacs, H., Gelencser, A., Hoffer, A., Kiss, G., Horvath, K., and Hartyani, Z.: Quantitative assessment of organosulfates in size-segregated rural fine aerosol, Atmospheric Chemistry and Physics, 9, 231-238, http://doi.org/10.5194/acp-9-231-2009, 2009.

Olson, C. N., Galloway, M. M., Yu, G., Hedman, C. J., Lockett, M. R., Yoon, T., Stone, E. A., Smith, L. M., and Keutsch, F. N.: Hydroxycarboxylic Acid-Derived Organosulfates: Synthesis, Stability, and Quantification in Ambient Aerosol, Environmental Science & Technology, 45, 6468-6474, http://doi.org/10.1021/es201039p, 2011.

Riva, M., Barbosa, T. D., Lin, Y. H., Stone, E. A., Gold, A., and Surratt, J. D.: Chemical characterization of organosulfates in secondary organic aerosol derived from the photooxidation of alkanes, Atmospheric Chemistry and Physics, 16, 11001-11018, http://doi.org/10.5194/acp-16-11001-2016, 2016.

Romero, F. and Oehme, M.: Organosulfates - A new component of humic-like substances in atmospheric aerosols?, Journal of Atmospheric Chemistry, 52, 283-294, http://doi.org/10.1007/s10874-005-0594-y, 2005.

Shakya, K. M. and Peltier, R. E.: Investigating Missing Sources of Sulfur at Fairbanks, Alaska, Environmental Science & Technology, 47, 9332-9338, http://doi.org/10.1021/es402020b, 2013.

Shakya, K. M. and Peltier, R. E.: Non-sulfate sulfur in fine aerosols across the United States: Insight for organosulfate prevalence, Atmospheric Environment, 100, 159-166, http://doi.org/10.1016/j.atmosenv.2014.10.058, 2015.

481   Staudt, S., Kundu, S., Lehmler, H.-J., He, X., Cui, T., Lin, Y.-H., Kristensen, K., Glasius, M., Zhang, X.,

482   Weber, R. J., Surratt, J. D., and Stone, E. A.: Aromatic organosulfates in atmospheric aerosols: Synthesis,

483   characterization,   and   abundance,   Atmospheric   Environment,   94,   366-373,

484   http://doi.org/10.1016/j.atmosenv.2014.05.049, 2014.

485   Stone, E. A., Yang, L. M., Yu, L. Y. E., and Rupakheti, M.: Characterization of organosulfates in

486   atmospheric aerosols at Four Asian locations, Atmospheric Environment, 47, 323-329,

487   http://doi.org/10.1016/j.atmosenv.2011.10.058, 2012.

488   Stone, E. A., Hedman, C. J., Sheesley, R. J., Shafer, M. M., and Schauer, J. J.: Investigating the chemical

489   nature of humic-like substances (HULIS) in North American atmospheric aerosols by liquid

490   chromatography tandem mass spectrometry, Atmospheric Environment, 43, 4205-4213,

491   http://doi.org/10.1016/j.atmosenv.2009.05.030, 2009.

492   Surratt, J. D., Lewandowski, M., Offenberg, J. H., Jaoui, M., Kleindienst, T. E., Edney, E. O., and Seinfeld,

493   J. H.: Effect of acidity on secondary organic aerosol formation from isoprene, Environmental Science &

494   Technology, 41, 5363-5369, http://doi.org/10.1021/es0704176, 2007a.

495   Surratt, J. D., Chan, A. W. H., Eddingsaas, N. C., Chan, M. N., Loza, C. L., Kwan, A. J., Hersey, S. P.,

496   Flagan, R. C., Wennberg, P. O., and Seinfeld, J. H.: Reactive intermediates revealed in secondary organic

497   aerosol formation from isoprene, Proceedings of the National Academy of Sciences of the United States

498   of America, 107, 6640-6645, http://doi.org/10.1073/pnas.0911114107, 2010.

499   Surratt, J. D., Kroll, J. H., Kleindienst, T. E., Edney, E. O., Claeys, M., Sorooshian, A., Ng, N. L.,

500   Offenberg, J. H., Lewandowski, M., Jaoui, M., Flagan, R. C., and Seinfeld, J. H.: Evidence for

501   organosulfates in secondary organic aerosol, Environmental Science & Technology, 41, 517-527,

502   http://doi.org/10.1021/es062081q, 2007b.

503   Surratt, J. D., Gomez-Gonzalez, Y., Chan, A. W. H., Vermeylen, R., Shahgholi, M., Kleindienst, T. E.,

504   Edney, E. O., Offenberg, J. H., Lewandowski, M., Jaoui, M., Maenhaut, W., Claeys, M., Flagan, R. C.,

505   and Seinfeld, J. H.: Organosulfate formation in biogenic secondary organic aerosol, J. Phys. Chem. A,

506   112, 8345-8378, http://doi.org/10.1021/jp802310p, 2008.

507   Tolocka, M. P. and Turpin, B.: Contribution of Organosulfur Compounds to Organic Aerosol Mass,

508   Environmental Science & Technology, 46, 7978-7983, http://doi.org/10.1021/es300651v, 2012.

509   Zhang, Y.-Q., Ding, X., He, Q.-F., Wen, T.-X., Wang, J.-Q., Yang, K., Jiang, H., Cheng, Q., Liu, P., Wang,

510   Z.-R., He, Y.-F., Hu, W.-W., Wang, Q.-Y., Xin, J.-Y., Wang, Y.-S., and Wang, X.-M.: Observational

511   Insights into Isoprene Secondary Organic Aerosol Formation through the Epoxide Pathway at Three

512   Urban Sites from Northern to Southern China, Environmental science & technology,

513   http://doi.org/10.1021/acs.est.1c06974, 2022.